

## Article

# Experimental Investigations of a Single-Slope Solar Still: Energy and Exergy Analysis

Haider Ali <sup>1</sup>, Sajid Ali <sup>2,\*</sup>, Sikandar Khan <sup>3,\*</sup> and Muhammad Umar Siddiqui <sup>4</sup>

<sup>1</sup> Department of Mechanical Engineering, Nadirshaw Eduljee Dinshaw (NED) University of Engineering & Technology, Karachi 75270, Pakistan

<sup>2</sup> Mechanical and Energy Engineering Department, Imam Abdulrahman Bin Faisal University, Dammam 31441, Saudi Arabia

<sup>3</sup> Department of Mechanical Engineering, King Fahd University of Petroleum and Minerals, Dhahran 31261, Saudi Arabia

<sup>4</sup> Department of Mechatronic Engineering, SZABIST University, 100 Clifton Block 5, Karachi Campus, Karachi 75270, Pakistan; dr.umarsiddiqui@szabist.edu.pk

\* Correspondence: sakzada@iau.edu.sa (S.A.); sikandarkhan@kfupm.edu.sa (S.K.)

**Abstract:** Fresh water is one of the prime necessities of a society; however, its availability is becoming a major concern with the increasing population. There are not enough sources of fresh water at present due to the high rate of population increase. Many regions worldwide face limited access to fresh water. Given economic limitations, there is an urgent need to create and market technologies enabling households to generate their fresh water. In areas with abundant solar energy and proximity to seawater or well-water sources, solar still technology, if developed and commercialized, offers a cost-effective solution for freshwater needs. Thus, the current study is focused on exploring the potential of solar stills for producing fresh water. A single-slope solar still is designed, fabricated and experimentally tested for the production of fresh water. The results of the analysis indicate a maximum production of 2.88 L/day with an energy efficiency of 52.42% and an exergetic efficiency of 7.04%. Overall, the current study reveals significant potential in utilizing solar stills for producing fresh water, which could be increased further if research is conducted on modifying its basic design to increase its productivity.



**Citation:** Ali, H.; Ali, S.; Khan, S.; Siddiqui, M.U. Experimental Investigations of a Single-Slope Solar Still: Energy and Exergy Analysis. *Energies* **2023**, *16*, 7659. <https://doi.org/10.3390/en16227659>

Academic Editor: Armando Oliveira

Received: 5 October 2023

Revised: 5 November 2023

Accepted: 15 November 2023

Published: 19 November 2023



**Copyright:** © 2023 by the authors. Licensee MDPI, Basel, Switzerland. This article is an open access article distributed under the terms and conditions of the Creative Commons Attribution (CC BY) license (<https://creativecommons.org/licenses/by/4.0/>).

**Keywords:** desalination; solar still; energy analysis; exergy analysis; fresh water; renewable energy

## 1. Introduction

Access to fresh water is an absolute necessity for the well-being of any society. As technological advancements have enhanced our quality of life, they have also led to an escalating demand for fresh water per individual. This growing need for fresh water, combined with the surging global population, has created a critical challenge: the scarcity of fresh water, particularly in densely populated urban areas. Take, for example, Karachi, one of Pakistan's most densely inhabited cities and home to approximately 16.7 million people [1], where the freshwater sources for such a huge population are still the same as they were 2 to 3 decades ago. As a result, currently, there are many areas in Karachi where fresh water is available only for few hours each week, while in other areas people are forced to use saline water for household activities. Thus, there is an immediate need to find solutions that could be technically feasible, economical and on a small scale so that an average household can easily implement them and be able to share the burden of the government. A focus of many researchers has been the application of solar energy to address the global issue of water scarcity [2–6].

One of the most feasible solutions for the production of fresh water is a solar still. A solar still is easy to manufacture and install; requires saline water, which is abundantly

available in Karachi, being a seaport; and requires solar energy, which is also available as Karachi receives  $6.05 \text{ kWh/m}^2/\text{day}$  of solar intensity on average [7].

Although being one of the simplest devices, the commercial solar still has not gained much attention due to very low freshwater output. So, most of the research about solar stills has been focused on modifying the basic design to increase fresh water production. For instance, Shukla and Modi [8] modified the design of solar still by utilizing a double basin with the upper basin having a dual slope and the lower basin having a single slope. While operating under hybrid mode, they reported a production of  $1.17 \text{ L/m}^2/\text{day}$  from the upper basin and  $0.28 \text{ L/m}^2/\text{day}$  of fresh water from the lower basin at an efficiency of 29.96%. Essa et al. [9] attempted to enhance the evaporation inside a solar still by introducing two rotating discs with wicks on the biggest wall inside a single-slope solar still. The experimental results of their analysis indicated an increase in the freshwater production from  $2.03 \text{ L/m}^2/\text{day}$  to  $3.15 \text{ L/m}^2/\text{day}$  (124% increase) for their proposed design.

Instead of having a single absorber basin, Chen et al. [10] modeled and experimentally tested a seawater desalination solar still that consisted of multiple trays stacked over one another. They reported that it took about 3 h for the system to move from transient-state to steady-state water production with a production of about  $8.1 \text{ L/m}^2/\text{day}$  and an efficiency of 112% for a seawater depth of 2 cm. Xie et al. [11] proposed a tubular solar still-type multi-effect desalination operating under vacuum pressure. Operating under vacuum pressure allows desalination at lower temperatures compared to standard design. The simulation of their design was validated against experimental results. They reported a production of  $17.2 \text{ kg/m}^2/\text{day}$  for a desalination system with an array of  $5 \times 5$  tubular cells with an overall efficiency of more than 70% at an estimated cost of USD 6.1/t of fresh water.

A few studies are focused on using solar stills in other systems for increasing overall energy utilization and the efficiency of such systems. For instance, Sharshir et al. [12] utilized a solar still to increase the efficiency and output of a humidification–dehumidification seawater desalination system. The results of their analysis indicated an output of about 37 L/day with an increase in the water production of 242% compared to a conventional design. Sharshir et al. [13], later on, also tested the integration of four solar stills with their system. They reported a water production of about 66.3 L/day using four solar stills.

Other approaches to increase the output of solar stills involve using thermoelectric systems, an external condenser and nanofluids within the solar stills. A rather comparatively more complicated system was tested by Parsa et al. [14]. They used silver nanoparticles along with thermo-electric heating integrated with a solar still and an external condenser. The results of their analysis indicated a water production of about  $7.76 \text{ L/m}^2/\text{day}$  with an increase in efficiency of about 100.5% for their design compared to a conventional solar still. Rahbar and Esfahani [15] designed and experimentally tested a solar still integrated with a thermoelectric module. The thermoelectric module was integrated to act as a cooler with its cold side enhancing the temperature difference between evaporation and condensation zones of the solar still whereas the hot side of the module was connected to a heat pipe cooling device for heat rejection. The results of their analysis indicated a very low productivity of fresh water (i.e.,  $180 \text{ L/m}^2/\text{year}$ ) compared to a pyramid-shaped solar still (i.e.,  $1533 \text{ L/m}^2/\text{year}$ ).

The addition of reflectors, side mirrors and external solar collectors represent other ways of increasing the performance of solar stills. For instance, Patel et al. [16] experimentally tested the performance of a double-slope solar still with reflectors on each slope side, integrated with an external condenser and a vacuum pump. They reported a freshwater production of 11.499 L/day and 8.212 L/day for summer and winter seasons, respectively, for their proposed design with a  $2 \text{ m}^2$  basin area. Sadeghi and Nazari [17] experimentally analyzed the use of an antibacterial nanofluid within a solar still equipped with an external evacuated solar collector and a thermoelectric cooling device. The results of their analysis indicated an increase in the freshwater production from  $2.75 \text{ L/m}^2/\text{day}$  to  $5.64 \text{ L/m}^2/\text{day}$  (218% increase) for their proposed design with a calculated cost of USD0.019/L/ $\text{m}^2$  of fresh water production for the proposed design at that time.

Bataineh and Abbas [18] theoretically and experimentally studied the performance of a solar still when nanoparticles, i.e.,  $\text{Al}_2\text{O}_3$  or  $\text{SiO}_2$ , were added to saline water under vacuum pressure. They reported a production of 1.518 kg/day (13% increase) and 1.510 kg/day (12% increase) of fresh water for a 1% concentration of  $\text{Al}_2\text{O}_3$  or  $\text{SiO}_2$ , respectively, for a  $0.36 \text{ m}^2$  solar still. Later, they also investigated the effect of adding internal reflectors and rectangular fins on the performance of the solar still [19]. They reported no significant effect on the performance of a solar still due to the addition of fins alone. The reason is that although the fins increase the absorption area, the shadow of the fins reduces the absorption area at the same time, thus nullifying the effect of fins. However, for a design with fins when combined with the internal reflectors, a production of  $3.014 \text{ L/m}^2/\text{day}$  (29.1% increase) of fresh water was achieved.

Sohani et al. [20] experimentally investigated the effect of employing side mirrors and solar tracking on the performance of active and passive solar stills. They reported a fresh water production of 2.19 L/day (43.1% increase) and 6.92 L/day (22.2% increase) for passive and active systems, respectively. Abdelmaksoud et al. [21] experimentally investigated the effect of introducing a photovoltaic-powered circulation pump and electric heater on the performance of a solar still. They reported a production of  $4.2 \text{ L/m}^2/\text{day}$  (24% increase) of fresh water with an estimated benefit–cost ratio of 4.1 for their design.

A novel design was proposed by Bouzaid et al. [22], which involved the use of an inclined basin with baffles as rectangular fins on the absorbing base plate. The baffles increased the absorption surface area, whereas the inclination of the basin allowed for lower water depth in the basin, resulting in an increased evaporation for higher freshwater production. The results of their analysis indicated a production of  $1.6 \text{ kg/m}^2/\text{h}$  of fresh water for an insolation of  $900 \text{ W/m}^2$ ; however, the analysis was conducted numerically without any experimental validation for their design. The idea of an inclined-basin solar still was experimentally tested by Abujazar et al. [23]. However, instead of using baffles, they used copper-stepped trays inside the inclined basin. They reported a freshwater production of  $4.383 \text{ L/m}^2/\text{day}$  with a capital cost of USD 0.047 for their proposed design.

Another attempt at increasing the freshwater production of a solar still was made by introducing a separate solar collector with the solar still equipped with phase change material [24,25]. The phase change material allows an extended time for production of fresh water, whereas the separate solar collector contributed to heating the saline water in the basin as well as the phase change material. Experiments on this design showed a production of  $4.3 \text{ L/m}^2/\text{day}$  of fresh water, out of which 40% was produced after sunset. Aqlan et al. [26] proposed a single-slope solar still where the saline water is directly heated in a parabolic trough solar collector and returned to a solar still for evaporation. The results of their experiments showed an increase in freshwater production from  $0.38 \text{ L/m}^2/\text{h}$  to  $0.67 \text{ L/m}^2/\text{day}$  (77% increase) for their proposed design. Khanmohammadi and Khanjani [27] proposed the use of hydrophobic glass within solar still in order to increase freshwater production. A cold plasma coat was used to convert the condensing glass of a solar still into hydrophobic glass. Experiments performed over a  $0.512 \text{ m}^2$  solar still indicated a 25.7% increase in the production of fresh water from 485 mL/day (for uncoated glass) to 610 mL/day (for the coated glass).

Various studies in the literature have discussed the economic and environmental aspects of designing solar stills. One such study was conducted on a cascade solar still desalination system [28], using tri-objective optimization involving total annual cost, exergy efficiency and a reduction in carbon emission. The results of their analysis indicated that a solar still that uses paraffin as a phase change material and glass wool as insulation has the lowest total annual cost. Asbik et al. [29] theoretically presented an exergy analysis of a solar still integrated with paraffin wax as a phase change material for heat storage. They concluded that integrating phase change material in a solar still increases the production of fresh water but decreases the exergetic efficiency of the solar still. In contrast, Mousa et al. [30] reported an overall decrease in the production of fresh water due to the use of a phase change material in the solar still. They reported a decrease in the production

of fresh water from 627 mL/day to 550 mL/day due to the inclusion of a phase change material within a 0.2542 m<sup>2</sup> solar still.

El-bar and Hassan [31] attempted an increase in the output of a solar still by employing saline water preheating and using a porous material within the solar still. The saline water was preheated by using it as a coolant for a solar photovoltaic panel, whereas black steel-wool fibers were used as a porous material inside the solar still. They reported a production of 3.534 kg/m<sup>2</sup>/day of fresh water (51.4% increase) with an efficiency of 38.07% for their design (38% increase) compared to a conventional solar still. A similar idea with a more complicated design was proposed by Mahmoud et al. [32], which involved the use of two solar photovoltaic panels with concentrators for preheating saline water as well as circulating air in the solar still. They reported a production of 9 kg/m<sup>2</sup>/day of fresh water at optimal operating conditions for their design. Later, Mahmoud et al. [33] modified their design by integrating it with the Glaubers salt as the phase change material with a 0.1 volume fraction of CuO nanoparticles. The results of their analysis indicated a production of 11.6 L/m<sup>2</sup>/day of fresh water for their modified design, showing a significant improvement in the output compared to the previous design. Kumar et al. [34] discussed the synthesis of CoO@ZnO nanostructures on Ni foam for use in supercapacitors, demonstrating excellent capacitance retention and suggesting potential applications in various energy-related technologies. Moniruzzaman [35] introduced a novel method for creating a highly efficient cobalt-doped @MnO<sub>2</sub> nanocomposite on conductive nickel foam for supercapacitors, improving specific capacitance and stability through enhanced electron transport pathways and multi-active electrochemical sites.

Kabeel et al. [36] used an array of hollow circular fins on absorber base plate of a pyramid-shaped solar still integrated with paraffin wax (phase change material) beneath the absorber plate as thermal storage for an extended operation time of freshwater production. Their experimental results indicated an increase in freshwater production from 4.02 L/m<sup>2</sup>/day to 5.75 L/m<sup>2</sup>/day (43% increase) due to the use of hollow circular fins, which further increased to 8.1 L/m<sup>2</sup>/day (101.5% increase) when integrated with a phase-change material as well. In another attempt to increase the production of solar stills, Kabeel [37] used a concave surface as an absorption plate of a pyramid-shaped solar still instead of a flat surface in combination with a jute wick. The jute wick increased evaporation due to the capillary effect, whereas the concave surface increased evaporation by increasing the surface area. The freshwater production experimentally reported was increased from 2.1 L/m<sup>2</sup>/day to 4.1 L/m<sup>2</sup>/day (95% increase) for the proposed design with a calculated cost of USD 0.065/L of freshwater production for the proposed design at that time.

Looking at context of freshwater availability in Pakistan, although a few freshwater rivers flow through Pakistan, due to the large overall population and extremely densely populated cities, the freshwater availability still remains an issue of concern within the country. In addition, there are regions where no fresh water is available at all, i.e., Baluchistan province. However, the availability of large solar energy and being close to seawater present the possibility of producing fresh water using solar stills. In this regard, Amjad and Shah [38] identified clusters of solar farms in the Baluchistan province of Pakistan that could be potential sites for the installation of solar-powered systems.

Unfortunately, very few studies are available that explore the potential of solar energy for producing fresh water in Pakistan. For instance, Samee et al. [39] experimentally tested the performance of a basic solar still in Islamabad, which was designed for an annual optimal solar tilt of 33.3°. They reported a production of 3.148 L/m<sup>2</sup>/day with an efficiency of 30.65%. Jamil et al. [40] theoretically designed and experimentally tested a pyramid-shaped solar still in the Rahim Yar Khan region of Pakistan. They reported a production of 1.5 L/m<sup>2</sup>/day of fresh water from their designed solar still fabricated at a capital cost of less than USD 20.

Malik et al. [41] theoretically evaluated the performance of three different designs for solar flash desalination plants operating under vacuum pressure. Real-time solar data for

Karachi was used in the theoretical analysis. Among the three designs, the one with heat recovery from the brine solution as well as the fresh water were reported to be the most suitable options. The results of their analysis indicated production rate, energy efficiency and exergy efficiency of 133 L/day, 68% and 12%, respectively. Besides the aforementioned research, to the best of the authors' knowledge, there is no specific literature available regarding the experimental exploration of the potential of solar stills for producing fresh water and conducting exergy analysis for Karachi city. Therefore, the present research is dedicated to evaluating the potential of solar stills for freshwater production, including energy and exergy analysis.

## 2. Materials and Methods

### 2.1. Design of Solar Still

A solar still is a simple device that utilizes solar energy to produce fresh water. Figure 1 shows a single-slope solar still. It is composed of a glass housing that allows smaller wavelength solar radiations (A) to enter the solar still but does not allow larger wavelength radiations to escape the glass housing, thus producing a high temperature within the solar still due to the greenhouse effect. The roof of the solar still, which is made of glass, is tilted at a specific slope to allow the maximum possible direct solar radiations to enter the solar still. As the solar radiations fall on the glass roof of the solar still, a small fraction of it is reflected out by the glass (B), a part of it is absorbed by the glass (C), while the remaining part enters the solar still. The sides of the solar still are made up of glass as well. The glass sides allow the shorter wavelengths coming from direct radiations to enter the solar still, especially during dawn and dusk. However, longer wavelength radiations are not able to escape the solar still due to the greenhouse effect. Thus, the glass sides help in augmenting the heat storing capacity of the solar still, eventually increasing the clean water production from it.

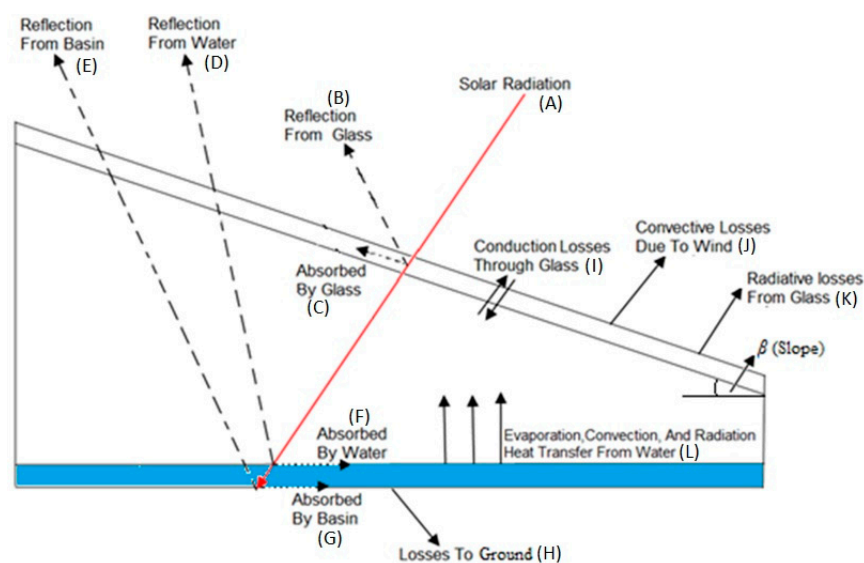


**Figure 1.** Heat transfer in a single-slope solar still.

If brackish water (saline water) is placed inside the basin of the solar still, a part of the solar energy will also be reflected by the brackish water (D) as well as the basin material (E). There will also be some losses of energy to the ground (H), whereas the remaining solar energy that has entered the solar still will be absorbed by the brackish water (F) and the basin (G). This absorbed solar energy by the brackish water causes evaporation inside the solar still (L). The evaporated water is pure (without any contamination) and is drawn out by convection to come into contact with the inner surface of the glass roof. Thus, the inner surface of the glass housing, being in contact with the evaporated water, is at a comparatively higher temperature. The outer surface of the glass housing is at a comparatively lower temperature, being in contact with outside air. Hence, the temperature

gradient between the inner and outer surfaces of the glass housing allows conduction heat transfer (I), resulting in the condensation of pure water, which is then collected as fresh water. During the process, a small fraction of energy is lost by the convective losses (J) due to the wind and the radiative losses from the glass (K). The left-over brackish water inside the basin of the solar still becomes more concentrated and is later removed and replaced with new brackish water.

## 2.2. Mathematical Modeling

Predicting the output and performance of a solar still requires mathematical modeling validated by experimental results. Mathematically, solar still performance is evaluated by the thermal analysis of the system. The thermal analysis includes heat transfer calculations performing energy and exergy balance, resulting in evaluating the efficiency of the system. However, the performance of such systems is strongly dependent on solar radiation data and the ambient conditions which behave as input parameters within this mathematical model. The following assumptions are made while developing the code to evaluate the energetic and exergetic performance of the solar still [42]:

- (i) Steady-state conditions occur during the time interval (steady operation over an hour).
- (ii) No vapor can escape from the still (no vapor leakage).
- (iii) The heat capacity of the glass cover, thermoelectric module surface and basin liner is negligible.
- (iv) The level of saline water remains constant in the basin.

### 2.2.1. Heat Transfer Calculations

Heat transfer phenomena for a single-slope solar still can be broadly categorized as (a) heat transfer on the internal surfaces and (b) heat transfer on the external surfaces.

The heat transfer on the internal surfaces of the solar still occurs inside the basin due to radiation, evaporation and convection. The convection heat transfer occurs between water and the glass housing due to the presence of humid air in the still. Convection heat transfer depends upon the water temperature ( $T_w$ ) and the temperature of the inner surface of the glass housing ( $T_{gi}$ ) represented by the following Equation (1) [43]

$$q_{c,w,gi} = h_{c,w,gi}(T_w - T_{gi}) \quad (1)$$

where  $h_{c,w,gi}$  is the convection heat transfer coefficient, which is calculated from Equation (2)

$$h_{c,w,gi} = 0.884 \left[ T_w - T_{gi} + (P_w - P_{gi}) \left( \frac{T_w + 273.15}{268900 - P_w} \right) \right]^{\frac{1}{3}} \quad (2)$$

where  $P_w$  and  $P_{gi}$  are the saturation pressure of water vapor and inner pressure of glass housing, respectively, which are calculated as follows:

$$P_w = \exp \left[ 25.317 - \left( \frac{5144}{T_w + 273} \right) \right] \quad (3)$$

$$P_{gi} = \exp \left[ 25.317 - \left( \frac{5144}{T_{gi} + 273} \right) \right] \quad (4)$$

Now, for radiation heat transfer, Equation (5) is derived by adopting the methodology used in [44]

$$q_{r,w,gi} = h_{r,w,gi}(T_w - T_{gi}) \quad (5)$$

where  $h_{r,w,gi}$  is the radiative heat transfer coefficient which is given by Equation (6) as

$$h_{r,w,gi} = \varepsilon_{eff} \sigma (T_w^2 + T_{gi}^2) (T_{gi} + T_w) \quad (6)$$

with effective emissivity given as

$$\varepsilon_{eff} = \left[ \frac{1}{\varepsilon_w} + \frac{1}{\varepsilon_g} - 1 \right]^{-1} \quad (7)$$

Similarly, the rate of evaporative heat transfer ( $q_{e,w,gi}$ ) inside the solar still can be calculated using Equation (8), with the evaporative heat transfer coefficient ( $h_{e,w,gi}$ ) given by Equation (9).

$$q_{e,w,gi} = h_{e,w,gi}(T_w - T_{gi}) \quad (8)$$

$$h_{e,w,gi} = 0.016273h_{c,w,gi} \left[ \frac{P_w - P_{gi}}{T_w - T_{gi}} \right] \quad (9)$$

The next step is to calculate the heat transfer from the external surfaces of the solar still. The majority of the heat losses from the solar still constitute heat transfer on external surfaces. While the solar still is composed of a glass housing (top surface) on a water basin (bottom surface), the majority of the heat losses from external surfaces represent heat losses from the top and bottom surfaces of the solar still.

First, the conductive heat transfer on the glass housing is calculated as

$$q_{cd,gi,go} = \frac{k_g}{L_g} (T_{gi} - T_{go}) \quad (10)$$

Applying energy balance at the outer surface of the glass housing, the amount of heat conducted to the outer glass surface is equal to the combined effect of convective and radiative heat transfer from the outer surface of the glass to the ambient.

$$q_{cd,gi,go} = q_{c,go,a} + q_{r,go,a} \quad (11)$$

Convective and radiative heat losses from the surfaces are given by Equations (12) and (13), respectively,

$$q_{c,go,a} = h_{c,go,a}(T_{go} - T_a) \quad (12)$$

$$q_{r,go,a} = h_{r,go,a}(T_{go} - T_a) \quad (13)$$

where the radiative coefficient of heat transfer ( $h_{r,go,a}$ ) are given by Equation (14),

$$h_{r,go,a} = \varepsilon \sigma \left[ \frac{(T_{go} + 273)^4 - (T_{sky} + 273)^4}{T_{go} - T_a} \right] \quad (14)$$

Although there is insulation at the bottom surface of the solar still, there are still some ground losses from the bottom of the solar still. These heat losses are determined by the following equations:

$$q_w = h_w(T_b - T_w) \quad (15)$$

$$q_b = h_b(T_b - T_a) \quad (16)$$

where  $h_b$ , which is the conductive heat transfer coefficient, is given as

$$h_b = \left[ \frac{L_{ins}}{k_{ins}} + \frac{1}{h_{t,b,a}} \right]^{-1} \quad (17)$$

and where  $h_{t,b,a}$  depends on the velocity of the air ( $V$ ) and is calculated as

$$h_{t,b,a} = 5.7 + 3.8V \quad (18)$$

### 2.2.2. Energy Balance

The energy balance is applied at the inner surface of the glass housing to determine the amount of heat received by the glass housing. It is also applied at the basin liner to calculate the amount of heat loss from the basin liner.

#### Inner Surface of Glass Housing

The energy balance at the inner surface of the glass housing is given by Equation (19)

$$q_{cd,gi,go} = \alpha_{d,g}I_t + q_{c,w,gi} + q_{e,w,gi} + q_{r,w,gi} \quad (19)$$

where  $I_t$  is the intensity of the sun on an inclined surface of glass housing which is given by

$$I_t = I \cos \beta_g \quad (20)$$

where  $I$  is the solar radiation's intensity and  $\beta_g$  is the solar angle of incidence for the glass cover. The term  $\alpha_{d,g}$  in Equation (19) represents the fractional solar flux of glass, which is given as

$$\alpha_{d,g} = (1 - R_g)\alpha_g \quad (21)$$

#### Basin Liner

The energy balance at the basin liner is given by Equation (22)

$$\alpha_{d,b}I_t = q_w + q_b \quad (22)$$

Substituting the values of  $q_w$  and  $q_b$  from Equations (15) and (16) into the Equation (22) gives

$$\alpha_{d,b}I_t = h_w(T_b - T_w) + h_b(T_b - T_a) \quad (23)$$

where

$$\alpha_{d,b} = ((\alpha_b(1 - \alpha_g)(1 - R_g))(1 - R_w)(1 - \alpha_w)) \quad (24)$$

### 2.2.3. Solar Radiation

The effect of inclination of the glass housing of the solar still as well as the conversion of standard time into solar time are evaluated by simultaneously solving Equations (25)–(30).

$$R_S = \frac{\cos \theta}{\cos \theta_z} \quad (25)$$

$$\text{Solar Time} - \text{Standard Time} = 4*(L_{st} - L_{LOC}) + E \quad (26)$$

$$E = 229.2 * (0.000075 + 0.001868 * \cos B - 0.032077 * \sin B - 0.014615 * \cos 2B - 0.04089 * \sin 2B) \quad (27)$$

$$\delta = 23.45 * \sin(360 * \frac{284 + n}{365}) \quad (28)$$

$$\begin{aligned} \cos \theta &= \sin \delta \sin \phi \cos \beta - \sin \delta \cos \phi \sin \phi \cos \gamma + \\ &\cos \delta \cos \phi \cos \beta \cos \omega + \cos \delta \sin \phi \sin \beta \cos \gamma \cos \omega \\ &+ \cos \delta \sin \beta \sin \lambda \sin \omega \end{aligned} \quad (29)$$

$$\cos \theta_z = \cos \phi \cos \delta \cos \omega + \sin \phi \sin \delta \quad (30)$$

### 2.2.4. Productivity Rate and Solar Still Efficiency

The productivity rate ( $m$ ) for the solar still is given by Equation (31)

$$m = \frac{q_{e,w,gi}}{\mathcal{L}} \quad (31)$$

where

$$\mathcal{L} = 2256 \times 10^3 \text{ J/kg} \quad (32)$$

The efficiency ( $\eta$ ) of a solar still is the ratio of the energy utilization for the production of water to the total energy input, Equation (33):

$$\eta = \frac{m\mathcal{L}}{I_t A_s} \quad (33)$$

### 2.2.5. Solar Still Exergetic Efficiency

The overall exergy efficiency of the solar still ( $\eta_{Ex}$ ), i.e., the exergy output associated with the distillate water to the solar exergy input, is given by

$$\eta_{Ex} = \frac{\text{Exergy output of Solar Still}}{\text{Exergy input of Solar Still}} = \frac{E_{x_{evap}}}{E_{x_{input}}} \quad (34)$$

where  $E_{x_{evap}}$  is the exergy related to evaporation and  $E_{x_{input}}$  is the exergy related to solar radiation and is given as

$$E_{x_{evap}} = mL \left( 1 - \frac{T_a}{T_w} \right) \quad (35)$$

$$E_{x_{input}} = A_s I_t \left[ 1 - \frac{4}{3} \left( \frac{T_a}{T_s} \right) + \frac{1}{3} \left( \frac{T_a}{T_s} \right)^4 \right] \quad (36)$$

### 2.3. Experimental Setup

An experimental setup is developed to test the performance and output of a single-slope solar still under the climatic conditions of Karachi. Figure 2a shows the Computer-Aided Design (CAD) model of the experimental setup, which contains all components of the solar still. In order to make it a standalone system, a PV panel is also attached. A pump and storage tank are added into the system along with a small electric board for controlling the pump and recording the reading. Figure 2b presents the actual experimental setup developed based on the CAD model for testing the solar still, which contains temperature sensors.



**Figure 2.** (a) CAD model of experimental setup and (b) actual experimental setup.

The experimental setup is developed in-house using a glass with a thickness of 1 cm. The slope of the glass housing should be able to collect most of the direct radiations throughout the year. However, this would require a solar tracking system, which would increase the operational complexity as well as reduce the economic feasibility of the solar still, so a fixed slope is selected for the design. The slope of glass housing is based on the latitude of Karachi. Since it has been well established that the slope of a fixed solar collector should be made equal to the latitude of the installed location for year-round operation, and given the solar still is being installed in Karachi, which has a latitude of around  $24.8^\circ$ , the experimental setup is developed with a  $25^\circ$  glass housing slope. The total area of the inclined glass surface is  $1.5 \text{ m}^2$ , which receives the input solar radiation. The basin is designed to hold a water depth of 4 cm. The inlet water temperature is  $25^\circ \text{C}$ . The basin is placed on an insulator base of 0.3 cm. Solar photovoltaic (PV) panels are used to power the pumps needed to ensure the continuous supply of brackish water and removal of fresh water as well as concentrated waste. The whole setup is placed on a movable metallic frame. Table 1 lists the main design parameters of the manufactured single-slope solar still.

**Table 1.** Design parameters for single-slope solar still.

Parameter	Value
Glass thickness ( $L_g$ )	0.01 m
Area of glass ( $A_g$ )	$1 \times 1.5 \text{ m}^2$
Slope	$25^\circ$
Solar collector (PV panel)	$32 \times 14$ inch
PV panel power	30 W
Depth of water ( $D$ )	0.04 m
Temperature inlet ( $T_{in}$ )	$25^\circ \text{C}$
Thickness of insulator ( $L_{ins}$ )	0.003 m

### 3. Results and Discussion

In order to study the performance of a single-slope solar still for producing fresh water, an in-house MATLAB code was developed to solve the equations discussed in the mathematical modeling section (Section 3). The properties of the glass used in the design as well as the properties of water and insulation are listed in Table 2.

**Table 2.** Properties used in the design.

Parameter	Value
Thermal conductivity of glass ( $K_g$ )	$1 \text{ W/m}^2\text{K}$
Emissivity of glass ( $\epsilon_g$ )	0.1
Absorptivity of glass ( $\alpha_g$ )	0.1
Reflectivity of glass ( $R_g$ )	0.2
Thermal conductivity of insulator ( $K_{ins}$ )	$0.038 \text{ W/m}^2\text{K}$
Emissivity of water ( $\epsilon_w$ )	0.1
Reflectivity of water ( $R_w$ )	0.02
Absorptivity of water ( $\alpha_w$ )	0.8
Absorptivity of basin ( $\alpha_b$ )	0.8
Latent heat of vaporization ( $\mathcal{L}$ )	2400 kJ/kg

In order to check the accuracy of the developed mathematical code, the estimated rate of freshwater production from the simulation is compared with the actual freshwater

yield of the experimental setup. Figure 3 shows a comparison of simulation (calculated from Equation (31)) and experimental results for freshwater production on 8 June 2022. The results of the analysis indicated that the simulation results are in good agreement with the experimental results, achieving an accuracy of approximately 96.8%. This instills confidence in the mathematical modeling. Therefore, the results of the analysis will provide a realistic direction for others.

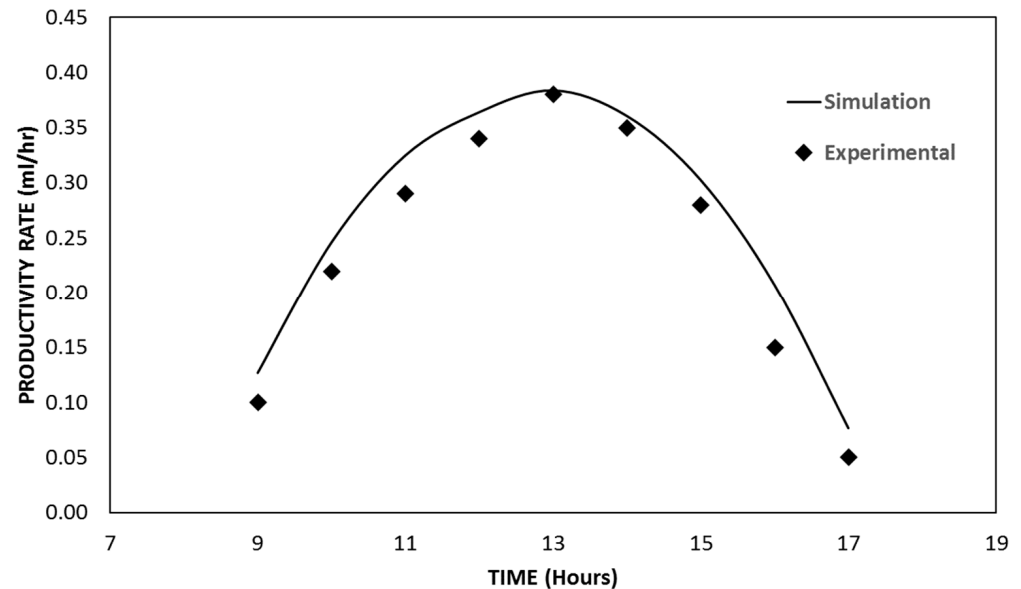


**Figure 3.** Comparison of simulation and experimental results for 8 June 2022.

Real-time solar radiation data for Karachi are obtained from the NED weather station and used as an input within the simulation. Figure 4 displays the solar radiation data for Karachi on four significant dates in 2022, 16 March, 11 June, 15 September and 10 December, chosen as representatives of their respective months. Notably, the solar radiation intensity remains relatively consistent from March to September. However, there is a decline in solar radiation intensity during December, typical for the winter season. This observation underscores that for the majority of the year, Karachi's climate offers an ideal environment for harnessing solar energy.

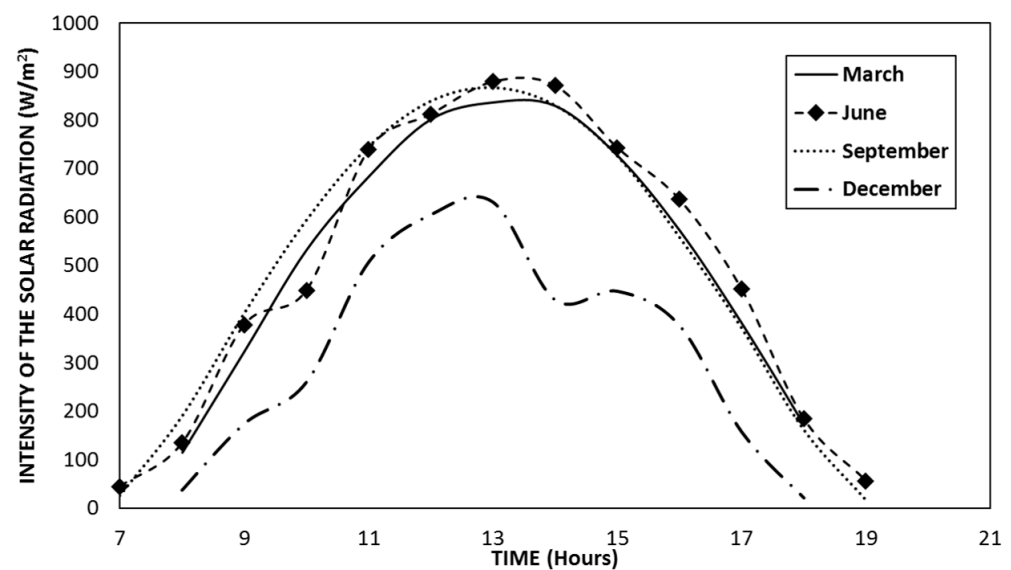


**Figure 4.** Intensity of solar radiation for 16 March, 11 June, 15 September and 10 December for 2022.

Figure 5 shows the simulated results for the hourly freshwater production rate (L/h), calculated from Equation (31), of the single-slope solar still for 16 March, 11 June, 15 September and 10 December. It can be seen from Figure 5 that during the month of September, peak hour freshwater production reaches up to 0.42 L/h. The large variability in the hourly fresh water production for the month of December corresponds to high winds and rainy weather.

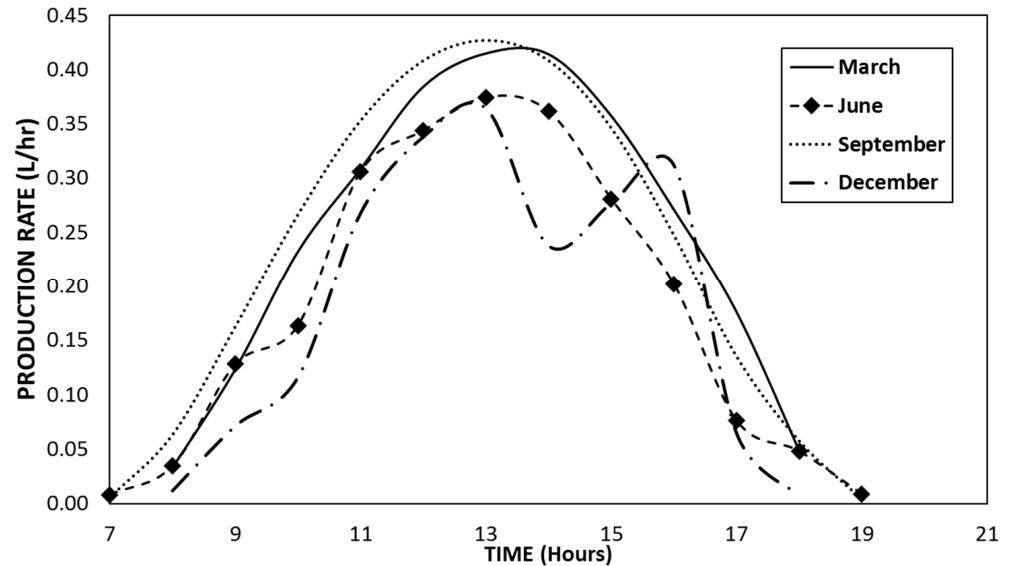


Figure 5. Production rate (L/h) for 16 March, 11 June, 15 September and 10 December for 2022.

Another critical parameter for assessing the performance of the single-slope solar still is the cumulative freshwater production, measured in liters. Figure 6 illustrates the cumulative production of fresh water in liters for the designed single-slope solar still. When examining Figures 5 and 6, it becomes clear that the peak cumulative freshwater production occurs in September, reaching 2.88 L per day. Conversely, the lowest cumulative production is observed in December, with a decline in freshwater output to approximately 2.06 L per day. This reduction in freshwater production in December corresponds with the decrease in available solar energy during that month, as depicted in Figure 4.

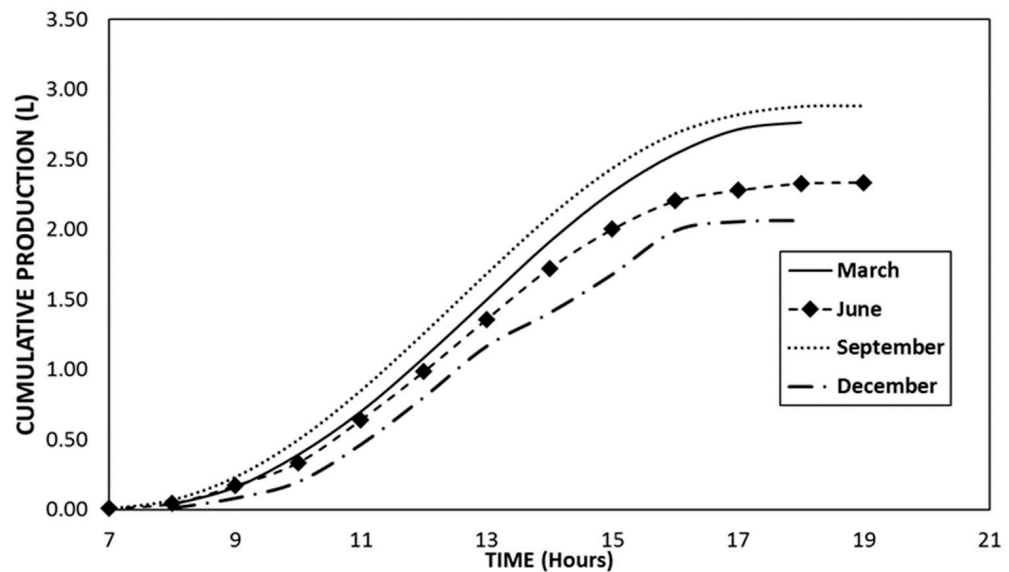


Figure 6. Cumulative production (L) for 16 March, 11 June, 15 September and 10 December for 2022.

Along with evaluating the usefulness of a single-slope solar still by determining the freshwater production, it is equally important to investigate the energy-wise performance of the device. Figure 7 shows the energy efficiency (calculated using Equation (33)) of the solar still. It can be seen from Figure 7 that the maximum efficiency ranges from 50.16% to 52.42% for the year 2022. Given that the tested solar still is of a basic design without any modifications for performance enhancement (i.e., reflectors, concentrators, etc.), the energetic efficiency of the single-slope solar still is found to be satisfactory and presents good potential for further device performance enhancement in future using modified designs.

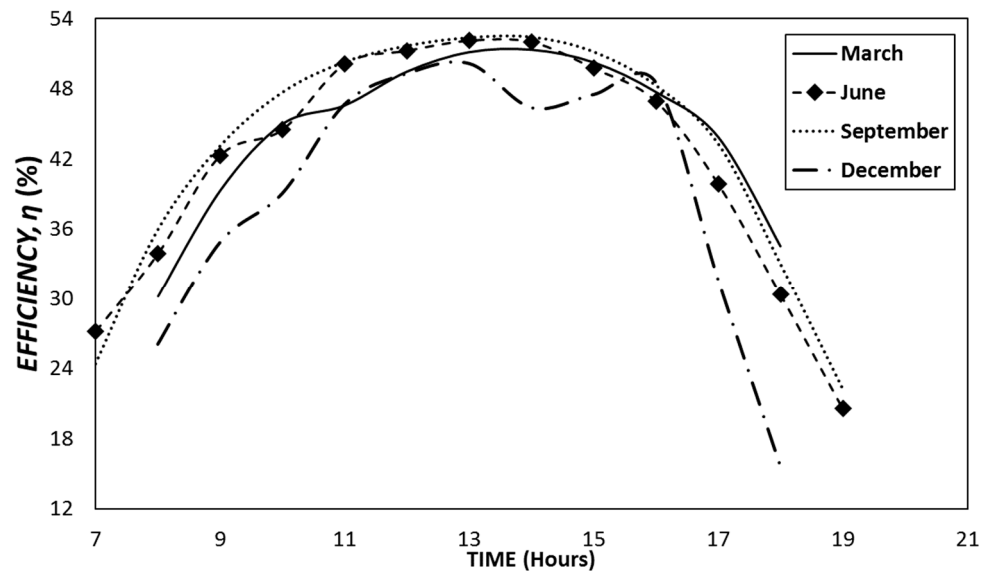


Figure 7. Energy efficiency for 16 March, 11 June, 15 September and 10 December for 2022.

While it is important to evaluate how well the energy is used by the device to produce the desired output using first law or energetic efficiency, it is equally important to estimate the utilizability of the device and available resources by estimating the second law or exergetic efficiency of the device as well. Figure 8 shows the exergetic efficiency (calculated from Equation (34)) of the solar-still for 16 March, 11 June, 15 September and 10 December. It can be seen from Figure 8 that the maximum exergetic efficiency is 7.04% in the month of March. The low value of exergetic efficiency shows that there are significant exergetic losses within the components of a single-slope solar still due to its simple design, and it presents significant potential for modifying the basic design to improve the solar still's exergetic efficiency in future studies.

When evaluating the cumulative daily fresh water production for the designed single-slope solar still using the developed mathematical model, it can be seen from Figure 9 that this device is capable of producing more than 2 L/day of fresh water steadily over the whole year, with the maximum cumulative fresh water production reaching 2.88 L/day in September and minimum freshwater production being 2.06 L/day in December.

This presents potential for the possible commercialization of the product, which might significantly contribute to the overall well-being of society and reduce the government's burden regarding the provision of fresh water to large populations in big cities.

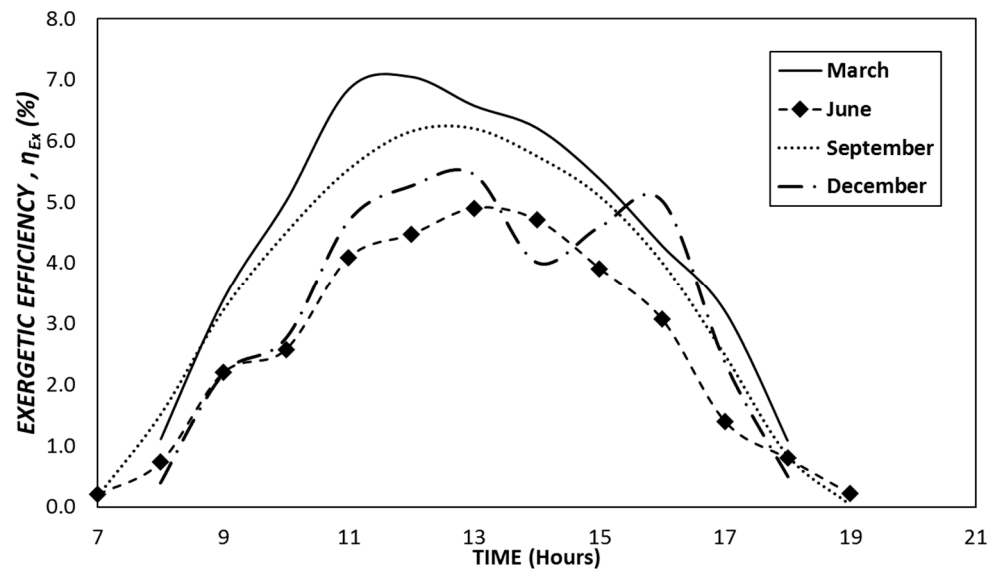


Figure 8. Exergetic efficiency for 16 March, 11 June, 15 September and 10 December for 2022.

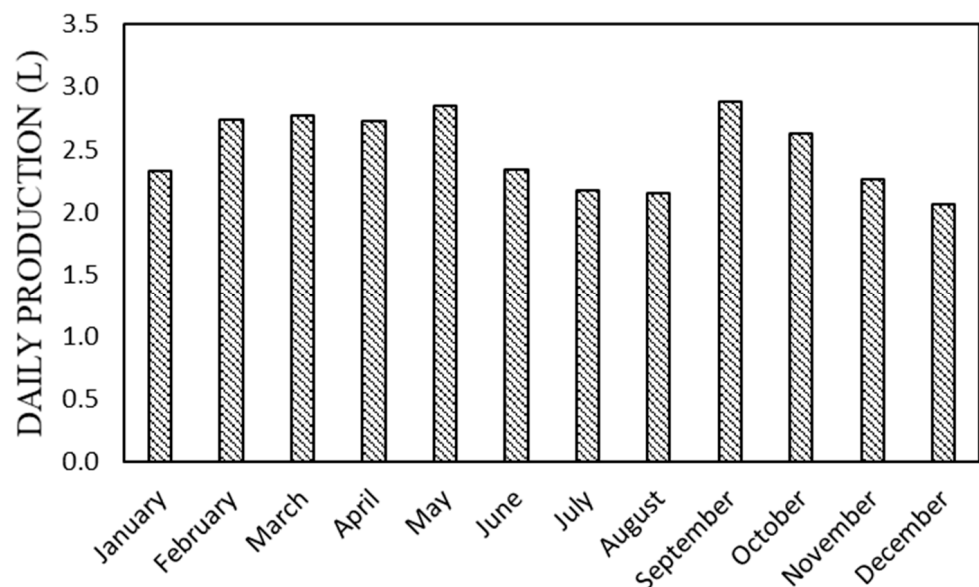


Figure 9. Daily fresh water production (L) for representative days of months for the year 2022.

#### 4. Comparison of Similar Studies

Table 3 provides an overview of various studies on freshwater production in different countries. The prevailing seawater desalination technologies encompass thermal desalination and membrane desalination methods. Within thermal desalination, three main techniques are prominent: multi-stage flash (MSF), multi-effect distillation (MED) and vapor compression (VC) desalination. The three primary types of membrane desalination are reverse osmosis (RO), forward osmosis (FO) and electrodialysis (ED). For instance, the 'Ayoun Mosa' (MSF) facility in Sinai, Egypt, boasts a capacity of 10,000 m<sup>3</sup>/day and can yield brine at 29 °C with a salinity of 48,000 ppm from saltwater feed. The El Sokhna desalination project in El Sokhna, Egypt, employs two distillation units to produce 8000 m<sup>3</sup>/day of clean water [45]. In Jubail, Saudi Arabia, the Al Fatah Water and Power project features the Jubail Seawater Reverse Osmosis Plant (RO), which draws 28.54 million m<sup>3</sup> of filtered water annually through a coastal well intake structure. Additionally, the Yanbu-2 seawater desalination plant in Yanbu Industrial City, located 300 km north of Jeddah, utilizes a multiple-effect distillation (MED) desalination unit to generate 43.84 million m<sup>3</sup> of fil-

tered water annually [46]. Moving to India, the Minjur desalination facility can produce 100,000 m<sup>3</sup> daily using reverse osmosis (RO) technology [47], and the Nemilli Desalination Plant in Nemmeli, situated on the shore of Chennai City, has a daily capacity of 93,000 m<sup>3</sup> through RO technology [48]. The Karachi Nuclear Power Plant (KANUPP) nuclear desalination plant offers a daily capacity of 4550 m<sup>3</sup> using MSF technology [49]. Most of the desalination techniques such as multiple-effect distillation, reverse osmosis, multi-stage flash, etc., require a large electrical input to run. However, considering the power shortage situation in Karachi, such systems are not suitable for operation in Karachi. Since a single-slope solar still does not require electrical input, this method is being considered in this study for freshwater production in Karachi.

**Table 3.** Comparison of similar studies.

S. No	Authors Name and Year	Plant	Location	Type of Experiment	Yield (m <sup>3</sup> /Day)
1	Yasser et al. [45]	Ayoun Mosa	Sinai, Egypt	Multi-stage flash	10,000
2	Yasser et al. [45]	El Sokhna	El Sokhna, Egypt	Multiple-effect distillation	8000
3	Omar Ouda [46]	Jubail RO	Jubail, Saudi Arabia	Reverse osmosis	178,560
4	Omar Ouda [46]	Yanbu 2	Yanbu, Saudi Arabia	Multiple-effect distillation	68,190
5	Water Technology Projects [47]	Minjur	Chennai, India	Reverse osmosis	100,000
6	Nemmeli desalination plant [48]	Nemilli	Chennai, India	Reverse osmosis	93,000
7	Khan & Khan [49]	KANUPP	Karachi, Pakistan	Multi-stage flash	4550

## 5. Conclusions

In this study, we evaluated the performance of a single-slope solar still through design, fabrication and experimental testing. A mathematical model was developed to simulate the device's performance, validated against experimental results. The findings indicate a maximum daily freshwater production of 2.88 L for a 1.5 m<sup>2</sup> single-slope solar still, with an energy efficiency of 52.42% and an exergy efficiency of 7.04%. During September, peak hourly freshwater production reached 0.42 L/h. Year-round variation in cumulative freshwater production was less than 1 L/day. Maximum production occurred in September at 2.88 L/day, while the minimum was in December at around 2.06 L/day. This study serves as a foundation for the development of domestic solar stills, with potential for commercialization, particularly through design enhancements.

**Author Contributions:** Conceptualization, H.A., M.U.S., S.A. and S.K.; methodology, H.A., M.U.S., S.A. and S.K.; software, H.A., M.U.S., S.A. and S.K.; validation, H.A., M.U.S., S.A. and S.K.; formal analysis, H.A., M.U.S. and S.A.; investigation, H.A., M.U.S. and S.A.; resources, H.A., M.U.S., S.A. and S.K.; data curation, H.A., M.U.S., S.A. and S.K.; writing—original draft preparation, H.A., M.U.S., S.A. and S.K.; writing—review and editing, H.A., M.U.S., S.A. and S.K.; visualization, H.A., M.U.S., S.A. and S.K.; supervision, H.A. and M.U.S.; project administration, H.A.; funding acquisition, H.A. All authors have read and agreed to the published version of the manuscript.

**Funding:** This research received no external funding.

**Data Availability Statement:** The data presented in this study are available upon request from the corresponding authors.

**Acknowledgments:** The authors wish to acknowledge the support of the NED University of Engineering and Technology, Shaheed Zulfiqar Ali Bhutto Institute of Science and Technology (SZABIST) University, Imam Abdulrahman Bin Faisal University (IAU) and King Fahd University of Petroleum and Minerals (KFUPM) by providing all the essential resources to conduct this study. In addition, the authors also acknowledge the support of Minhaj, Faaraz, Muzammil and Khawar in this experimental work.

**Conflicts of Interest:** The authors declare no conflict of interest.

## Nomenclature

CAD	Computer-Aided Design
PV	Photovoltaic
NED	Nadirshaw Eduljee Dinshaw
MSF	Multi-Stage Flash
MED	Multi-Effect Distillation
VC	Vapor Compression
RO	Reverse Osmosis
FO	Forward Osmosis
ED	Electrodialysis
KANUPP	Karachi Nuclear Power Plant

## References

1. Karachi, Pakistan Population (2022)—Population Stat. Available online: <https://populationstat.com/pakistan/karachi> (accessed on 7 March 2022).
2. Ali, S.; Al-Amri, F.; Saeed, F. Numerical and Experimental Performance Evaluation of a Photovoltaic Thermal Integrated Membrane Desalination System. *Energies* **2022**, *15*, 7417. [CrossRef]
3. Hariri, N.G.; Almutawa, M.A.; Osman, I.S.; Almadani, I.K.; Almahdi, A.M.; Ali, S. Experimental Investigation of Azimuth- and Sensor-Based Control Strategies for a PV Solar Tracking Application. *Appl. Sci.* **2022**, *12*, 4758. [CrossRef]
4. Al-Amri, F.; Maatallah, T.S.; Al-Amri, O.F.; Ali, S.; Ali, S.; Ateeq, I.S.; Zachariah, R.; Kayed, T.S. Innovative Technique for Achieving Uniform Temperatures across Solar Panels Using Heat Pipes and Liquid Immersion Cooling in the Harsh Climate in the Kingdom of Saudi Arabia. *Alex. Eng. J.* **2022**, *61*, 1413–1424. [CrossRef]
5. Siddiqui, M.U.; Ali, S.; Khan, S.; Ali, S.; Horoub, M.M. Optimum Tilt Angles of Solar Collectors in Saudi Arabia. In Proceedings of the 2021 International Conference on Electrical, Communication, and Computer Engineering (ICECCE), Kuala Lumpur, Malaysia, 12–13 June 2021. Available online: <https://ieeexplore.ieee.org/document/9514079> (accessed on 4 October 2023).
6. Khan, S.; Ahmad, N. Renewable Energy Generation and Storage. In *Sustainable Energy Storage for Furthering Renewable Energy*; Begell House: Danbury, CT, USA, 2022. [CrossRef]
7. PVWatts Calculator. Available online: <https://pvwatts.nrel.gov/pvwatts.php> (accessed on 7 March 2022).
8. Shukla, D.; Modi, K. Hybrid Solar Still as a Co-Generative System and Desalination System—An Experimental Performance Evaluation. *Clean. Eng. Technol.* **2021**, *2*, 100063. [CrossRef]
9. Essa, F.A.; Abdullah, A.S.; Omara, Z.M. Rotating Discs Solar Still: New Mechanism of Desalination. *J. Clean. Prod.* **2020**, *275*, 123200. [CrossRef]
10. Chen, Z.; Peng, J.; Chen, G.; Hou, L.; Yu, T.; Yao, Y.; Zheng, H. Analysis of Heat and Mass Transferring Mechanism of Multi-Stage Stacked-Tray Solar Seawater Desalination Still and Experimental Research on Its Performance. *Sol. Energy* **2017**, *142*, 278–287. [CrossRef]
11. Xie, G.; Sun, L.; Mo, Z.; Liu, H.; Du, M. Conceptual Design and Experimental Investigation Involving a Modular Desalination System Composed of Arrayed Tubular Solar Stills. *Appl. Energy* **2016**, *179*, 972–984. [CrossRef]
12. Sharshir, S.W.; Peng, G.; Yang, N.; El-Samadony, M.O.A.; Kabeel, A.E. A Continuous Desalination System Using Humidification—Dehumidification and a Solar Still with an Evacuated Solar Water Heater. *Appl. Therm. Eng.* **2016**, *104*, 734–742. [CrossRef]
13. Sharshir, S.W.; Peng, G.; Yang, N.; Eltawil, M.A.; Ali, M.K.A.; Kabeel, A.E. A Hybrid Desalination System Using Humidification-Dehumidification and Solar Stills Integrated with Evacuated Solar Water Heater. *Energy Convers. Manag.* **2016**, *124*, 287–296. [CrossRef]
14. Parsa, S.M.; Rahbar, A.; Koleini, M.H.; Aberoumand, S.; Afrand, M.; Amidpour, M. A Renewable Energy-Driven Thermoelectric-Utilized Solar Still with External Condenser Loaded by Silver/Nanofluid for Simultaneously Water Disinfection and Desalination. *Desalination* **2020**, *480*, 114354. [CrossRef]
15. Rahbar, N.; Esfahani, J.A. Experimental Study of a Novel Portable Solar Still by Utilizing the Heatpipe and Thermoelectric Module. *Desalination* **2012**, *284*, 55–61. [CrossRef]
16. Patel, S.K.; Singh, D.; Devnani, G.L.; Sinha, S.; Singh, D. Potable Water Production via Desalination Technique Using Solar Still Integrated with Partial Cooling Coil Condenser. *Sustain. Energy Technol. Assess.* **2021**, *43*, 100927. [CrossRef]
17. Sadeghi, G.; Nazari, S. Retrofitting a Thermoelectric-Based Solar Still Integrated with an Evacuated Tube Collector Utilizing an Antibacterial-Magnetic Hybrid Nanofluid. *Desalination* **2021**, *500*, 114871. [CrossRef]
18. Bataineh, K.M.; Abbas, M.A. Improving the Performance of Solar Still by Using Nanofluids, Vacuuming, and Optimal Basin Water Thickness. *Desalination Water Treat.* **2020**, *173*, 105–116. [CrossRef]
19. Bataineh, K.M.; Abbas, M.A. Performance Analysis of Solar Still Integrated with Internal Reflectors and Fins. *Sol. Energy* **2020**, *205*, 22–36. [CrossRef]
20. Sohani, A.; Hoseinzadeh, S.; Berenjkari, K. Experimental Analysis of Innovative Designs for Solar Still Desalination Technologies; An in-Depth Technical and Economic Assessment. *J. Energy Storage* **2021**, *33*, 101862. [CrossRef]

21. Abdelmaksoud, W.; Almaghrabi, M.; Alruwaili, M.; Alruwaili, A. Improving Water Productivity in Active Solar Still. *Energy Sources Part A Recovery Util. Environ. Eff.* **2021**, *43*, 2774–2787. [[CrossRef](#)]
22. Bouzaid, M.; Ansari, O.; Taha-Janani, M.; Mouhsin, N.; Oubrek, M. Numerical Analysis of Thermal Performances for a Novel Cascade Solar Desalination Still Design. *Energy Procedia* **2019**, *157*, 1071–1082. [[CrossRef](#)]
23. Abujazar, M.S.S.; Fatihah, S.; Kabeel, A.E. Seawater Desalination Using Inclined Stepped Solar Still with Copper Trays in a Wet Tropical Climate. *Desalination* **2017**, *423*, 141–148. [[CrossRef](#)]
24. Al-harashseh, M.; Abu-Arabi, M.; Mousa, H.; Alzghoul, Z. Solar Desalination Using Solar Still Enhanced by External Solar Collector and PCM. *Appl. Therm. Eng.* **2018**, *128*, 1030–1040. [[CrossRef](#)]
25. Abu-Arabi, M.; Al-harashseh, M.; Mousa, H.; Alzghoul, Z. Theoretical Investigation of Solar Desalination with Solar Still Having Phase Change Material and Connected to a Solar Collector. *Desalination* **2018**, *448*, 60–68. [[CrossRef](#)]
26. Aqlan, A.M.; Aklan, M.; Momin, A.E. Solar-Powered Desalination, a Novel Solar Still Directly Connected to Solar Parabolic Trough. *Energy Rep.* **2021**, *7*, 2245–2254. [[CrossRef](#)]
27. Khanmohammadi, S.; Khanjani, S. Experimental Study to Improve the Performance of Solar Still Desalination by Hydrophobic Condensation Surface Using Cold Plasma Technology. *Sustain. Energy Technol. Assess.* **2021**, *45*, 101129. [[CrossRef](#)]
28. Khanmohammadi, S.; Khanmohammadi, S. Energy, Exergy and Exergo-Environment Analyses, and Tri-Objective Optimization of a Solar Still Desalination with Different Insulations. *Energy* **2019**, *187*, 115988. [[CrossRef](#)]
29. Asbik, M.; Ansari, O.; Bah, A.; Zari, N.; Mimmet, A.; El-Ghetany, H. Exergy Analysis of Solar Desalination Still Combined with Heat Storage System Using Phase Change Material (PCM). *Desalination* **2016**, *381*, 26–37. [[CrossRef](#)]
30. Mousa, H.; Naser, J.; Gujarathi, A.M.; Al-Sawafi, S. Experimental Study and Analysis of Solar Still Desalination Using Phase Change Materials. *J. Energy Storage* **2019**, *26*, 100959. [[CrossRef](#)]
31. Elbar, A.R.A.; Hassan, H. Enhancement of Hybrid Solar Desalination System Composed of Solar Panel and Solar Still by Using Porous Material and Saline Water Preheating. *Sol. Energy* **2020**, *204*, 382–394. [[CrossRef](#)]
32. Mahmoud, A.; Fath, H.; Ahmed, M. Enhancing the Performance of a Solar Driven Hybrid Solar Still/Humidification-Dehumidification Desalination System Integrated with Solar Concentrator and Photovoltaic Panels. *Desalination* **2018**, *430*, 165–179. [[CrossRef](#)]
33. Mahmoud, A.; Fath, H.; Ookwara, S.; Ahmed, M. Influence of Partial Solar Energy Storage and Solar Concentration Ratio on the Productivity of Integrated Solar Still/Humidification-Dehumidification Desalination Systems. *Desalination* **2019**, *467*, 29–42. [[CrossRef](#)]
34. Kumar, Y.A.; Kim, H.-J. Effect of Time on a Hierarchical Corn Skeleton-like Composite of CoO@ ZnO as Capacitive Electrode Material for High Specific Performance Supercapacitors. *Energies* **2018**, *11*, 3285. [[CrossRef](#)]
35. Moniruzzaman, M.; Anil Kumar, Y.; Pallavolu, M.R.; Arbi, H.M.; Alzahmi, S.; Obaidat, I.M. Two-Dimensional Core-Shell Structure of Cobalt-Doped@ MnO<sub>2</sub> Nanosheets Grown on Nickel Foam as a Binder-Free Battery-Type Electrode for Supercapacitor Application. *Nanomaterials* **2022**, *12*, 3187. [[CrossRef](#)]
36. Kabeel, A.E.; El-Maghlany, W.M.; Abdelgaied, M.; Abdel-Aziz, M.M. Performance Enhancement of Pyramid-Shaped Solar Stills Using Hollow Circular Fins and Phase Change Materials. *J. Energy Storage* **2020**, *31*, 101610. [[CrossRef](#)]
37. Kabeel, A.E. Performance of Solar Still with a Concave Wick Evaporation Surface. *Energy* **2009**, *34*, 1504–1509. [[CrossRef](#)]
38. Amjad, F.; Shah, L.A. Identification and Assessment of Sites for Solar Farms Development Using GIS and Density Based Clustering Technique- A Case of Pakistan. *Renew. Energy* **2020**, *155*, 761–769. [[CrossRef](#)]
39. Ali Samee, M.; Mirza, U.K.; Majeed, T.; Ahmad, N. Design and Performance of a Simple Single Basin Solar Still. *Renew. Sustain. Energy Rev.* **2007**, *11*, 543–549. [[CrossRef](#)]
40. Jamil, M.A.; Yaqoob, H.; Farooq, M.U.; Teoh, Y.H.; Xu, B.B.; Mahkamov, K.; Sultan, M.; Ng, K.C.; Shahzad, M.W. Experimental Investigations of a Solar Water Treatment System for Remote Desert Areas of Pakistan. *Water* **2021**, *13*, 1070. [[CrossRef](#)]
41. Malik, A.; Qureshi, S.R.; Abbas, N.; Zaidi, A.A. Energy and Exergy Analyses of a Solar Desalination Plant for Karachi Pakistan. *Sustain. Energy Technol. Assess.* **2020**, *37*, 100596. [[CrossRef](#)]
42. Dehghan, A.A.; Afshari, A.; Rahbar, N. Thermal Modeling and Exergetic Analysis of a Thermoelectric Assisted Solar Still. *Sol. Energy* **2015**, *115*, 277–288. [[CrossRef](#)]
43. Elango, C.; Gunasekaran, N.; Sampathkumar, K. Thermal Models of Solar Still—A Comprehensive Review. *Renew. Sustain. Energy Rev.* **2015**, *47*, 856–911. [[CrossRef](#)]
44. Hussein, A.K.; Rashid, F.L.; Abed, A.M.; Al-Khaleel, M.; Togun, H.; Ali, B.; Akkurt, N.; Malekshah, E.H.; Biswal, U.; Al-Obaidi, M.A.; et al. Inverted solar stills: A comprehensive review of designs, mathematical models, performance, and modern combinations. *Sustainability* **2022**, *14*, 13766. [[CrossRef](#)]
45. Elsaie, Y.; Soussa, H.; Gado, M.; Balah, A. Water Desalination in Egypt; Literature Review and Assessment. *Ain Shams Eng. J.* **2022**, *14*, 101998. [[CrossRef](#)]
46. Ouda, O.K.M. Domestic Water Demand in Saudi Arabia: Assessment of Desalinated Water as Strategic Supply Source. *Desalination Water Treat.* **2015**, *56*, 2824–2834.
47. Projects Archive—Water Technology. Available online: <https://www.water-technology.net/projects/> (accessed on 24 February 2023).

48. Nimmeli Desalination Plant: A Reliable Model for Coastal India—For Pure Water, Think WABAG! Available online: <https://www.wabag.com/project/nimmeli-desalination-plant-providing-sustainable-solutions-through-desalination/> (accessed on 24 February 2023).
49. Khan, S.U.-D.; Khan, S.U.-D. Karachi Nuclear Power Plant (KANUPP): As Case Study for Techno-Economic Assessment of Nuclear Power Coupled with Water Desalination. *Energy* **2017**, *127*, 372–380. [[CrossRef](#)]

**Disclaimer/Publisher’s Note:** The statements, opinions and data contained in all publications are solely those of the individual author(s) and contributor(s) and not of MDPI and/or the editor(s). MDPI and/or the editor(s) disclaim responsibility for any injury to people or property resulting from any ideas, methods, instructions or products referred to in the content.